P-Glycoprotein Senses Its Substrates and the Lateral Membrane Packing Density: Consequences for the Catalytic Cycle[†]

Päivi Äänismaa, Ewa Gatlik-Landwojtowicz, and Anna Seelig*

Biophysical Chemistry, Biozentrum, University of Basel, Klingelbergstrasse 70, Basel CH-4056, Switzerland

Received February 5, 2008; Revised Manuscript Received June 11, 2008

ABSTRACT: P-glycoprotein (ABCB1) prevents absorption (e.g., blood-brain barrier) or enhances excretion (e.g., kidney) by moving substrates from the cytosolic to the extracellular membrane leaflet at the expense of ATP hydrolysis. It translocates various drugs and functions in membranes exhibiting different lateral packing densities. To gain more functional insight, we measured the temperature dependence of the P-glycoprotein ATPase activity in NIH-MDR1-G185 cell membranes in the absence and presence of three drugs (promazine, verapamil, and PSC833), exhibiting significantly different transporter affinities. Activation enthalpies ($\Delta H^{\ddagger}$) and entropies ($T\Delta S^{\ddagger}$) were derived from Eyring plots. In the absence of drugs, the activation enthalpy and the free energy of activation for P-glycoprotein ATPase activity was determined as $\Delta H^{\ddagger} = 92.6 \pm 4.2$ kJ/mol and $\Delta G^{\ddagger} = 73.1 \pm 7.2$ kJ/mol, respectively. Increasing the drug concentration reduced the activation enthalpy, whereby the drug with the highest transporter affinity had the strongest effect ($\Delta\Delta H^{\ddagger} = -21\%$). The free energy of activation decreased for activating ($\Delta\Delta G^{\ddagger} = \sim -3.8\%$) and increased for inhibitory compounds ($\Delta\Delta G^{\ddagger} = \sim +0.7\%$). The drug-specific changes of the free energy of activation are thus barely above thermal energy. A comparison with literature data revealed that a decrease of the lateral membrane packing density reduces the enthalpic and the entropic contribution to the free energy of activation. Although the P-glycoprotein ATPase activity increases only slightly with decreasing lateral membrane packing density, the mode of action changes from strongly entropy-driven at high, to essentially enthalpy-driven at low packing densities. This suggests that the transporter and the membrane form a functional entity.

The human ATP binding cassette transporter, P-glycoprotein, Pgp[1] (MDR1, ABCB1), is highly expressed in absorptive membrane barriers such as the intestinal barrier and the blood−brain barrier where it reduces or even prevents absorption of drugs and toxins. It is also present in membranes of excretory organs such as the liver and the kidney, where it enhances excretion (for review see ref *1*). Moreover, it is abundant in many tumor cells contributing to multidrug resistance (MDR) (for review see ref *2*). The transporter (170 kDa) consists of two transmembrane domains (TMDs) each comprising six putative transmembrane helices and two nucleotide binding domains (NBDs) exposed to the cytosol. The latter dimerize upon nucleotide binding which leads to the formation of an outward-facing conformation by the TMDs (*3*).

The analysis of substrate binding and transport by Pgp is complex for several reasons. First, Pgp transports chemically very different compounds (*4*) at different rates (*5*–*7*). This is in contrast to most well-known transporters which move one single substrate or one class of substrates at a constant rate. An example for the latter case is the related heterodimer TAP1/TAP2 (ABCB2/ABCB3) associated with antigen processing (*8*).

Second, Pgp binds its substrates in the lipid membrane (*9*) and more precisely in the cytosolic membrane leaflet (*10*) and flips them to the outer leaflet, whereas most well-known transporters, including TAP1/TAP2 (*8*), bind and release their substrates in the aqueous phase. This implies that exogenous compounds have to cross the membrane by passive diffusion to reach the Pgp binding site. It also implies that the concentration of half-maximum activation depends on the nature of the lipid membrane (*11*).

Although transport by Pgp has long been suggested to correlate with ATP hydrolysis (*12*), the stoichiometry is still discussed. Compounds that diffuse rapidly across the membrane partially escape to the cytosol before they are caught by Pgp. Therefore, apparent transport tends to be lower than intrinsic transport (*13*). The direct correlation between transport and ATP hydrolysis was demonstrated using permanently charged compounds such as fluorescent dyes (*14*) or a spin-labeled verapamil analogue (*15*) that cannot cross the membrane by passive diffusion. However, these compounds partially remain bound to the extracellular membrane leaflet after transport, and therefore the question of whether one molecule of ATP is required to transport one substrate molecule (*16*) or whether two molecules are required as demonstrated for TAP1/TAP2 (*17*) is difficult to resolve. We quantified the apparent transport of drugs

[†] Funding provided by the Swiss National Science Foundation (Grant 3100AO-107793).

* Corresponding author. Phone: +41-61-267 22 06. Fax: +41-61-267 21 89. E-mail: Anna.Seelig@unibas.ch.

[1] Abbreviations: ABC, ATP binding cassette transporters in humans include seven subfamilies ABCA to ABCG; ECAR, extracellular acidification rate; MDR, multidrug resistance; NBD, nucleotide binding domain; Pgp, human P-glycoprotein-ATPase (MDR1, ABCB1); PGP1, hamster P-glycoprotein-ATPase; TMD, transmembrane domain.

10.1021/bi800209h CCC: $40.75
Published on Web 08/30/2008

across a cell membrane as the sum of passive influx and active efflux by Pgp, assuming that the rate of transport equals the rate of ATP hydrolysis. The excellent agreement with data from transport assays provided clear evidence for the direct correlation between the rate of ATP hydrolysis and the rate of effective transport by Pgp (*13, 18*).

Pgp ATPase activity was assessed by measuring the release of inorganic phosphate from inside-out plasma membrane vesicles and proteoliposomes (*5, 7, 19*) or by measuring the release of lactate from living cells (*11*). In the absence of drugs the Pgp ATPase shows basal activity. Upon titration with drugs the activity increases up to a maximum and then decreases again at high concentrations. The bell-shaped activity profiles have been analyzed by modified Michaelis−Menten kinetics (*5, 7, 11, 19*). The kinetic models used to evaluate the bell-shaped activity curves take into account an activating drug binding step at low and an inhibitory drug binding step at high concentrations, followed by a catalytic ATP hydrolysis step. These models provide an adequate description of the drug-induced variation of Pgp ATPase activity as discussed in detail elsewhere (*11*); however, the catalytic step includes further steps such as substrate translocation and transporter resetting. Despite extensive efforts it is still controversial whether ATP hydrolysis drives only the substrate translocation (*16, 19, 20*), only transporter resetting after release of the substrate (*21*), or both substrate translocation and transporter resetting (*22, 23*).

Insight into the reaction mechanism can be gained by measuring the temperature dependence of ATP hydrolysis rates which allows determination of the transition state parameters. The first comprehensive transition state analysis for Pgp and hamster P-glycoprotein (PGP1) was performed by Al-Shawi et al. (*19*). They determined the transition state parameters for ATPase activity in liposomes of different composition in the absence and presence of drugs and suggested that the activation enthalpy, $\Delta H^{\ddagger}$ (or activation energy, E_a), as a function of drug concentration first decreases and then increases (*19*). No or only negligibly small effects were observed by others (*5, 24, 25*).

The activation energies, E_a, reported for basal Pgp ATPase activity in various membranes or membrane mimicking systems differ significantly (*19, 24, 26*). Although several investigators have shown that Pgp senses the lipid composition (*19, 27*) and the phase state of the lipid membrane (*14*) the role of the lipid membrane in modulating basal Pgp ATPase activity has not yet been investigated systematically.

We therefore first analyzed how the drug, its concentration, and its affinity to the transporter influence the transition state parameters (i.e., the activation enthalpy, $\Delta H^{\ddagger}$, the activation entropy, $\Delta S^{\ddagger}$, and the free energy of activation, $\Delta G^{\pm}$) for Pgp ATPase activity. As test compounds we used promazine, verapamil, and the Pgp inhibitor PSC833, an analogue of cyclosporin A, which differ considerably in their affinity to the transporter (*11*). All three compounds are transported by Pgp, although only verapamil and PSC833 appear as substrates in transport assays (*13, 18*). As membrane system we used inside-out plasma membrane vesicles of NIH-MDR1-G185 cells. Second, we analyzed how the nature of the membrane influences the activity of the Pgp ATPase. To this purpose we compared the transition state parameters for basal Pgp ATPase activity in plasma membranes of NIH-MDR1-G185 cells with transition state parameters for basal Pgp ATPase activity in other systems. A meaningful comparison is possible if the Pgp ATPase containing membranes are characterized by the same physical chemical parameter. Parameters used to characterize lipid membranes are, e.g., fluidity, the order parameter, and the lateral membrane packing density. A decrease in fluidity generally correlates with an increase in the order parameter and the lateral membrane packing density. Here, we characterized the membranes in terms of the lateral packing density, π_M (*28, 29*), since it can be directly estimated from ATPase activity measurements (*11*).

Our investigation shows that all three drugs, even those which reduce the Pgp ATPase activity such as PSC833, reduced the activation enthalpy, $\Delta H^{\ddagger}$ (and the activation energy, E_a), for ATP hydrolysis, whereby the effect was considerable at high drug concentrations. The free energy of activation, $\Delta G^{\ddagger}$, for Pgp ATPase activity decreased at low and increased at high drug concentrations. The free energy of activation, $\Delta G^{\ddagger}$, for Pgp ATPase activity as a function of concentration thus yielded the mirror image of the bell-shaped activity profiles in good agreement with the Eyring theory. The comparison of the transition state parameters for Pgp ATPase activity in the different membrane systems revealed that the activation enthalpy, $\Delta H^{\ddagger}$, and the free energy of activation, $\Delta G^{\ddagger}$, for Pgp ATPase activity decrease with decreasing lateral membrane packing density, π_M, whereby the effect is significant in the former and small in the latter case. The catalytic cycle of the Pgp ATPase is discussed in the light of the present data.

MATERIALS AND METHODS

Materials. PSC833 was a gift from Novartis AG (Basel, Switzerland). Promazine·HCl was obtained from Sigma-Aldrich (Steinheim, Germany), (*R*/*S*)-verapamil·HCl from Fluka (Buchs, Switzerland), complete EDTA-free protease inhibitor cocktail tablets from Roche Diagnostics (Mannheim, Germany), 1,4-dithio-DL-threitol, DTT, from Applichem (Darmstadt, Germany), and bicinchoninic acid, BCA, protein assay reagents from Pierce (Rockford, IL). All other chemicals were either obtained from Sigma, Fluka, or Merck. Cell culture media DMEM with pyruvate (catalog no. 21969) as well as other compounds required for cell culture such as fetal bovine serum, FBS, L-glutamine, and antibiotics were purchased from Gibco-BRL (Basel, Switzerland).

Stock solutions for the phosphate release assay were made with nanopure water in the case of promazine and verapamil and with DMSO in the case of PSC833. The samples for measurements were prepared by adding 5 μL of the aqueous drug solution or 1 μL of the DMSO/drug solution to the phosphate release assay buffer (total sample volume per well = 60 μL). The final DMSO concentration was constant c = 1.7% (v/v).

NIH-MDR1-G185 Cells and the Corresponding Plasma Membrane Vesicles. Wild-type (NIH3T3) and MDR1-transfected mouse embryo fibroblasts (NIH-MDR1-G185) were generous gifts from Dr. M. M. Gottesman and Dr. S. V. Ambudkar (National Institutes of Health, Bethesda, MD). Cells were grown in the presence of 0.15 μM colchicine and were maintained as described previously (*30*). The crude plasma membrane vesicles were prepared as described in detail elsewhere (*7*).

Scheme 1: Pgp ATPase Activity at Low Substrate Concentration Considering One ATP Hydrolyzed per Cycle[a]

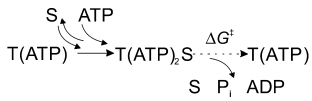

(1)

[a] See ref *16*. The dotted arrow indicates that the catalytic step is more complex than observed by Pgp ATPase measurements.

Monitoring Pgp ATPase Activity in Plasma Membrane Vesicles with Colorimetric Phosphate Release Assay. The Pgp-associated ATP hydrolysis was measured according to Litman et al. (*5*) in 96-well microtiter plates (Nunc F96 MicroWell plate, nontreated) with small modifications. Briefly, the plasma membrane vesicles were diluted to a protein concentration of 0.1 mg/mL in ice-cold phosphate release assay buffer (25 mM Tris-HCl including 50 mM KCl, 3 mM ATP, 2.5 mM $MgSO_4$, 3 mM DTT, 0.5 mM EGTA, 2 mM ouabain, and 3 mM sodium azide) unless otherwise stated. The buffer was adjusted to pH 7.0 at the respective temperatures by taking into account the temperature coefficient of the buffer. Each sample contained ~5 μg of protein per total assay volume of 60 μL. Incubation with drugs was started by transferring the plate from ice to a water bath kept at the temperature of choice for 1 h and was terminated by rapidly cooling the plate on ice. The inorganic phosphate, P_i, concentration was determined by addition of ice-cold solution (200 μL) containing ammonium molybdate (0.2% (w/v)), sulfuric acid (1.43% (v/v)), freshly prepared ascorbic acid (1% (w/v)), and SDS (0.9% (w/v)). After incubation at room temperature (30 min) the released phosphate was quantified colorimetrically at 820 nm using a Spectramax M2 (Molecular Device, Sunnyvale, CA). Reference phosphate standards were included to each 96-well plate. Samples incubated with 0.5 mM vanadate to determine the vanadate-sensitive Pgp activity were obtained in parallel and were subtracted from the measured values.

Reaction Mechanism. The basic reaction for ATP hydrolysis by Pgp at low drug concentration where only the activating binding region is occupied is shown in Scheme 1. The reaction including the second binding step is shown in detail elsewhere (*11*). The ATP-substrate stoichiometry is still discussed (see introduction). For simplicity we assume a stoichiometry of 1:1 as suggested previously (*16*). The transporter, T(ATP), binds the transport substrate, S (in the inner leaflet of the lipid membrane); moreover, it binds a second ATP molecule from the aqueous phase, yielding the transporter−ATP−substrate complex, $T(ATP)_2S$. The catalytic step includes ATP hydrolysis, the release of P_i, ADP, and substrate, and yields the starting complex T(ATP), where k is the measured catalytic rate constant, and $\Delta G^{\ddagger}$ is the corresponding free energy of activation. In the absence of drugs T(ATP) also binds a second molecule of ATP yielding the complex, $T(ATP)_2$; ATP is then hydrolyzed and the starting complex T(ATP) is formed.

Data Evaluation Using Modified Michaelis−Menten Kinetics. For data evaluation we used modified Michaelis−Menten kinetics (*5*) which considers two substrate binding steps

$$V_{sw} = \frac{K_1K_2V_{bas} + K_2V_1C_{sw} + V_2C_{sw}^{\ 2}}{K_1K_2 + K_2C_{sw} + C_{sw}^{\ 2}} \quad (1)$$

where V_{sw} is the rate of P_i release (Pgp ATPase activity) as a function of the substrate concentration in aqueous solution, C_{sw}, V_{bas} is the basal activity of Pgp in the absence of drugs, V_1 is the maximum transporter activity (if only activation occurred), and V_2 is the minimum activity at large substrate concentration. At a substrate concentration, K_1, half-maximum Pgp activation, and at a substrate concentration, K_2, half-maximum Pgp inhibition is reached. The catalytic rate constant, k_1, or turnover number corresponds to $V_1/[T]_0$, where $[T]_0$ is the transporter concentration. According to eq 1 the rate, V_{sw}, can be measured in the presence ($C_{sw} > 0$) or in the absence of substrates ($C_{sw} = 0$). In the absence of substrates the rate of the reaction corresponds to the basal rate ($V_{sw} = V_{bas}$). For practical reasons, i.e., to investigate the role of drug concentration, we further define $V_{sw}/[T]_0$ as k_{sw}.

Temperature Dependence of Pgp ATPase Activity and Evaluation of the Transition State Parameters. The bell-shaped activity curve described by eq 1 was measured in the present study as a function of temperature yielding the temperature dependence of the different rate parameters such as V_{sw} or k_{sw}. We evaluate the experimental data according to the Eyring equation (2)

$$k = \kappa\frac{k_BT}{h}e^{-\Delta G^{\ddagger}/RT} = \kappa\frac{k_BT}{h}e^{-\Delta H^{\ddagger}/RT}e^{\Delta S^{\ddagger}/R} \quad (2)$$

where κ is the transmission factor assumed to be unity, k_B is Boltzmann's constant, h Planck's constant, R the gas constant, T the absolute temperature, $\Delta G^{\ddagger}$ the free energy of activation, $\Delta S^{\ddagger}$ the activation entropy, and $\Delta H^{\ddagger}$ the activation enthalpy. It is assumed that all transition states break down with the same rate, k_BT/h. On the assumption that the entropy, $\Delta S^{\ddagger}$, of activation, the enthalpy, $\Delta H^{\ddagger}$, of activation, and the constant k_B are temperature independent and, moreover, a single process is monitored, a plot of $\ln(k/T)$ vs $1/T$ (Eyring plot) yields the activation enthalpy, from the slope and the activation entropy, $\Delta S^{\ddagger}/R$, from the y-axis intercept. This equation permits a calculation of the free energy of activation, $\Delta G^{\ddagger}$, from measured rate constants as

$$\Delta G^{\ddagger} = \Delta H^{\ddagger} - T\Delta S^{\ddagger} \quad (3)$$

The relationship between the activation enthalpy, $\Delta H^{\ddagger}$, and the activation energy, E_a, can be expressed as

$$\Delta H^{\ddagger} = E_a - RT \quad (4)$$

The Isokinetic Relationship. It was proposed that for any single rate-limiting transition state there is a linear free energy relationship between two rate constants for the reaction, k_{T_1} and k_{T_2}, measured at two different temperatures, ($T_1 < T_2$) (*19, 31*)

$$\ln k_{T2} = a + b \ln k_{T1} \quad (5)$$

where a and b are constants. A plot of $\ln k_{T_2}$ as a function of $\ln k_{T_1}$ yields a preliminary test of a common mechanism in related reactions. When the plots deviate from one another, it follows to a high probability that the mechanisms of the two related reactions are different.

Estimation of the Free Energies of Drug and ATP Binding to Pgp. The free energies of drug binding, $\Delta G^{\circ}_{tw(1)}$, were calculated from concentrations of half-maximum activity, K_1. Based on the assumption that the binding step is much faster

Table 1: Characteristic Parameters for Test Compounds and Transition State Parameters for ATP Hydrolysis by the Pgp ATPase in the Absence and Presence of Different Drugs

drug	MW_{base} (Da)	A_D[a] (Å^2)	K_1 (μM)	V_1 (%)	$\Delta G°_{tw(1)}$ (kJ/mol)	concn[d] (μM)	$\Delta H^{‡e}$ (kJ/mol)	$T\Delta S^{‡e}$ (37 °C) (kJ/mol)	$\Delta G^{‡e}$(37 °C) (kJ/mol)
basal						0	92.6 ± 4.2	19.5 ± 1.0	73.1
promazine	284.4	42	214.5 ± 28.6[b]	378 ± 15[b]	−31.2[b]	160.6	83.5 ± 6.5	11.9 ± 1.1	71.6
verapamil	454.6	90	1.0 ± 0.2	250 ± 28	−44.5	0.8	88.5 ± 12.7	17.2 ± 2.8	71.2
PSC833	1214.6	140	0.008 ± 0.001	84 ± 10	−56.6	1.9	73.4 ± 7.7	−0.2 ± 0.1	73.6
verapamil[c]			0.67 ± 0.09	274 ± 10	−45.6				

[a] The cross-sectional areas, A_D, were determined by surface activity measurements in 50 mM Tris-HCl and 114 mM NaCl, pH 8.0 at ambient temperature; the cross-sectional area, A_D, of PSC833 was assumed to be identical to that of cyclosporin A (*11*). The concentration of half-maximum Pgp activation, K_1, and the maximum Pgp activity, V_1, were determined at 37 °C and pH 7.0. [b] Data for promazine were obtained with a membranes prepared from older cells and gave higher values for the concentration of half-maximum Pgp activation, K_1, than given in ref *7*. [c] Measurements performed at pH 7.5, $T = 35$ °C. [d] Transition state data are given at the concentrations closest to the concentration of half-maximum activation, K_1, for promazine and verapamil and for the concentration of half-maximum inhibition, K_2, for PSC833. [e] The transition state parameters are evaluated from Figure 2. The parameters are apparent values and are valid in the given temperature range. The $\Delta G^{‡}$ values have to be considered as estimates. Thermodynamic parameters for basal values are the average of seven different temperature dependence measurements with multiple samples (number of samples, $n > 140$, four different membrane preparations). Thermodynamic parameters for drug-stimulated values are the average of one temperature dependence measurement with multiple samples. The errors for basal and drug-stimulated values represent the goodness of the linear fit.

than the subsequent catalytic step (*11*), K_1 can be considered as dissociation constant and the inverse $1/K_1$ as transporter-water binding constant, $K_{tw(1)}$ to a first approximation.

$$1/K_1 \cong K_{tw(1)} \quad (6)$$

The assumption made in eq 6 is supported by the similarity of the concentrations of half-maximum activation, K_m, for ATP hydrolysis and the dissociation constant, K_d, determined for ATP binding to MIANS-labeled Pgp. Moreover, the K_m for tetramethylrosamine also compared favorably with the K_d for MIANS-labeled Pgp (*14*).

The corresponding free energy relationship is

$$\Delta G°_{tw(1)} \cong -RT \ln(C_w K_{tw(1)}) \cong -RT \ln(C_w(1/K_1)) \quad (7)$$

The degree sign refers to a biological standard state (pH 7.4 and 37 °C), and $C_w = 55.3$ mol/L corresponds to the molar concentration of water at 37 °C. The constants $K_{tw(1)}$ and $1/K_1$ with the units L/mol are multiplied by the concentration of water, C_w (mol/L), to obtain mole fraction units (*32*). A corresponding expression was formulated for ATP binding:

$$\Delta G°_b = -RT \ln(C_w(1/K_m)) \quad (8)$$

RESULTS

Pgp ATPase Activity in Inside-Out Plasma Membrane Vesicles as a Function of Drug Concentration and Temperature. The test compounds, promazine, verapamil, and PSC833, are listed in Table 1 together with their molecular weight, cross-sectional area, A_D, concentration of half-maximum Pgp ATPase activation, K_1, maximum activity, V_1, and free energy of binding from water to the activating binding region of the transporter, $\Delta G°_{tw(1)}$. The more negative the free energy of binding, $\Delta G°_{tw(1)}$, the higher is the binding affinity to the transporter as shown previously (*11*). The molecular weight, the cross-sectional area, A_D, and the binding affinity to the transporter increase considerably in the order promazine < verapamil < PSC833, and the concentrations of half-maximum activation, K_1, differ by orders of magnitude.

The basal, V_{bas}, and drug-induced Pgp ATPase activity, V_{sw}, in inside-out vesicles formed from plasma membranes of NIH-MDR1-G185 cells were measured by monitoring the phosphate release rate with a colorimetric assay (*7*). Titrations were performed as a function of concentration at different temperatures over the temperature range, $\Delta T = 25-37$ °C, with the buffer adjusted to pH 7.0 at each temperature. The titration curves are shown in Figure 1.

The first point in each titration curve (Figure 1) corresponds to basal activity, V_{bas}, and the subsequent points to drug-induced ATPase activity, V_{sw}. The solid lines drawn in Figure 1 are fits to the measured data using the kinetic model given in eq 1. Each drug shows a specific ATPase activity profile that is characterized by four parameters (see eq 1), the concentration of half-maximum activation, K_1 (with one molecule bound to the transporter), the concentration of half-maximum inhibition, K_2 (with two molecules bound to the transporter), and the maximum, V_1, and minimum, V_2, ATPase activity, respectively (see also ref *5*). Promazine (Figure 1A) and verapamil (Figure 1B) exhibit the typical bell-shaped activity curves as a function of concentration, whereas PSC833 (Figure 1C) reduces the ATPase activity relative to basal values in the whole concentration range measured. With increasing temperature basal, V_{bas}, and drug-induced ATPase activity, V_{sw}, increase. However, the shape of the activity curves remains approximately constant for a given drug. For comparison with literature data (see below, Figure 8), we also measured the Pgp ATPase activity as a function of verapamil concentration at pH 7.5 (Tris buffer) and $T = 35$ °C (see Table 1). The concentration of half-maximum activation, K_1, is lower than at pH 7.0 due to the higher lipid−water partition coefficient, K_{lw}, of the drug at the higher pH; however, the maximum activity, V_1, is similar (Table 1).

The Thermodynamic Transition State Parameters for Pgp ATPase Activity in the Presence of Different Drugs. Figure 2 displays plots of $\ln(k_{sw}/T)$ vs the reciprocal absolute temperature (Eyring plot) in the absence and presence of drugs for inside-out plasma membrane vesicles of NIH-MDR1-G185 cells. Each line corresponds to a specific concentration in the activity profiles (Figure 1). The lines are linear fits to the data. The activation enthalpy, $\Delta H^{‡}$, and activation entropy, $\Delta S^{‡}$, for Pgp ATPase activity were determined from the slope and the *y*-axis intercept, respectively. The transition state parameters determined from Eyring plots are summarized in Table 1. As previously pointed out by Al-Shawi et al. (*19*), data derived from these

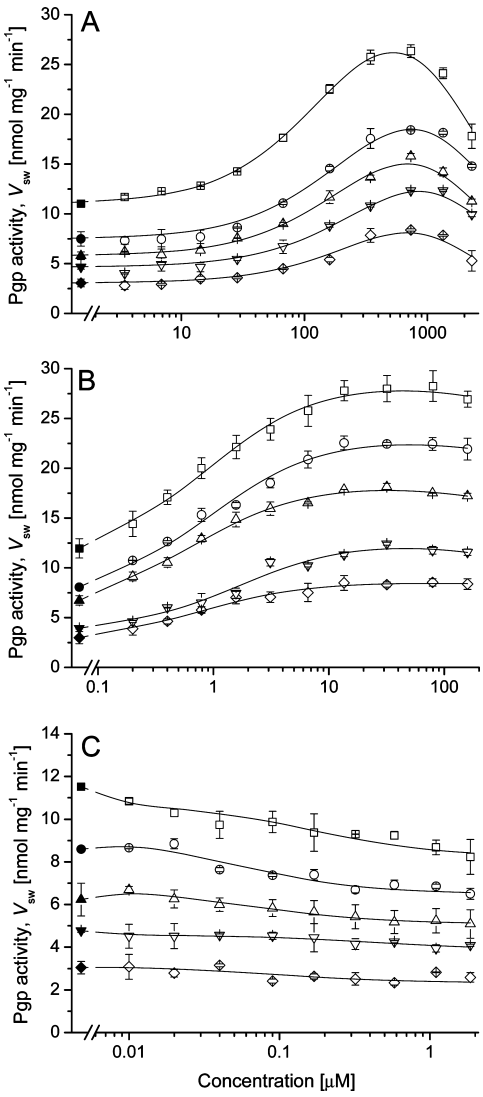

FIGURE 1: (A−C) Temperature dependence of the Pgp ATPase activity, V_{sw}, as a function of drug concentration in inside-out plasma membranes of NIH-MDR1-G185 cells: promazine (A), verapamil (B), and PSC833, an "inhibitor" of the Pgp ATPase (C). The filled and open symbols represent basal and drug-induced Pgp ATPase activity, respectively. Pgp ATPase activity was measured by means of a colorimetric phosphate release assay at (◆, ◇) 25, (▼, ▽) 28, (▲, △) 31, (●, ○) 34, and (■, □) 37 °C, either in 25 mM Tris-HCl or 25 mM Hepes−KOH buffer. Buffers were adjusted to pH 7.0, taking into account the temperature coefficient of the buffer. Data are expressed as the average of two to four experiments. Solid lines are fits to the modified Michaelis−Menten equation (eq 1).

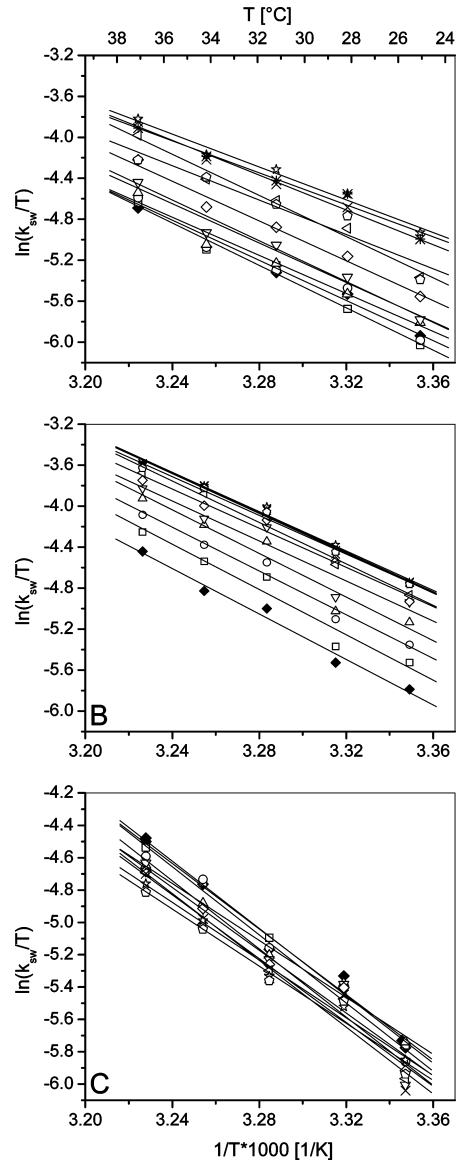

FIGURE 2: (A−C) Analysis of the thermodynamic transition state parameters by means of Eyring plots for Pgp ATPase activity in plasma membrane vesicles: Eyring plots for Pgp ATPase activity under basal conditions (◆) and increasing concentrations of promazine (A), verapamil (B), and PSC833 (C) (open symbols and stars). Each symbol corresponds to a specific concentration in Figure 1. Pgp ATPase activity is expressed in absolute values (s^{-1}) and was calculated as described previously (*7*). The amount of the Pgp ATPase in plasma membrane vesicle preparations used in verapamil and PSC833 measurements was estimated as 0.9% and in promazine measurements as 1.1% of total protein. The straight lines are linear fits to the data.

plots have to be considered as apparent values, valuable for the particular membrane and the temperature range indicated.

Figure 3 shows ln V_1 for promazine and verapamil as a function of the reciprocal absolute temperature. The maximum rate, V_1, is expressed relative to basal value at the corresponding temperature. In this representation the maximum rate, V_1, decreases with increasing temperature, because the change in activity with temperature is more pronounced in the absence than in the presence of drugs.

Transition State Parameters of the Pgp ATPase Activity as a Function of Drug Concentration. We have measured the transition state parameters for the Pgp ATPase activity in NIH-MDR1-G185 plasma membranes over a large range of concentrations (Figure 2) covering the full activity profiles (Figure 1). Figure 4A−C shows the thermodynamic transition state parameters, $\Delta H^{\ddagger}$, $T\Delta S^{\ddagger}$, and $\Delta G^{\ddagger}$, derived for Pgp ATPase activity as a function of promazine, verapamil, and PSC833 concentration, respectively. The concentration of half-maximum activation for promazine and verapamil and the concentration of half-maximum inhibition for PSC833 are indicated by arrows. In the absence of drugs the activation enthalpy for ATPase activity in plasma membrane vesicles of NIH-MDR1-G185 cells was determined as $\Delta H^{\ddagger} = 92.6 \pm 4.2$ kJ/mol. Increasing the drug concentration reduced the activation enthalpy, $\Delta H^{\ddagger}$, and the activation entropy, $T\Delta S^{\ddagger}$, for both activating and inhibitory compounds as seen in Figure 4A−C. The reduction in the enthalpy increased in the order verapamil ($\Delta\Delta H^{\ddagger} = -14$ kJ/mol) (−15%) <

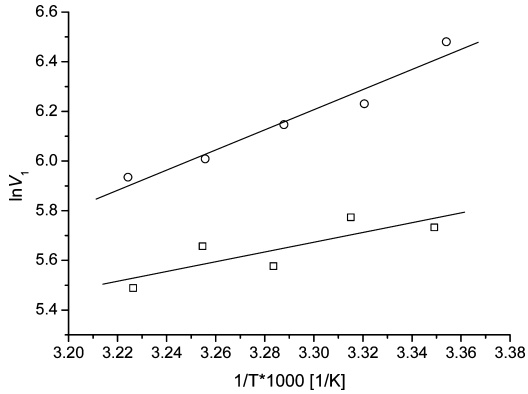

FIGURE 3: Temperature dependence of maximum Pgp ATPase activity, ln V_1 (where V_1 is given in % values), for verapamil (□) and promazine (○). The straight lines are the linear regressions to the data. Data are expressed as the average of two to six experiments.

PSC833 ($\Delta\Delta H^{\ddagger} = -19.2$ kJ/mol) (−21%) < promazine ($\Delta\Delta H^{\ddagger} = -27.6$ kJ/mol) (−30%) at the highest concentrations investigated. At high drug concentrations the entropy contribution almost vanished, and the Pgp ATPase was therefore essentially enthalpy driven under these conditions. Figure 4A−C shows that the drug-induced changes are not negligible as assumed previously (*5, 24, 25*) but depend on the drug concentration applied. Data in Figure 4A−C also differ from those observed by Al-Shawi et al. (*19*).

The free energy of activation was determined as $\Delta G^{\ddagger} = 73.1$ kJ/mol (at $T = 37$ °C) in the absence of drugs. With increasing promazine and verapamil concentration (Figure 4D,E) the free energy of activation, $\Delta G^{\ddagger}$, first decreased and then increased again, while it increased already at low concentrations of PSC833 (Figure 4F). The decrease relative to the basal value was $\Delta\Delta G^{\ddagger} = -2.8$ kJ/mol (−3.8%) for verapamil, and the increase relative to the basal value was $\Delta\Delta G^{\ddagger} = +0.5$ kJ/mol (+0.7%) for PSC833. The drug-induced changes in the free energy of activation, $\Delta G^{\ddagger}$, relative to basal values are thus small, but drug specific.

To test the relevance of the $\Delta G^{\ddagger}$ values, we inserted them into the Eyring equation (eq 2) and calculated the activity profiles (i.e., the rate constants, k_{sw}, as a function of concentration) for comparison with the ATPase activity profiles measured directly at a given temperature (Figure 4G−I). Since the $\Delta G^{\ddagger}$ values change with concentration, the calculated curve is not a simple exponential (see eq 2) but is indeed bell-shaped. The resulting activity profiles showed a 2−3-fold increase and a somewhat smaller decrease in rate depending on the concentration, in excellent agreement with the experimentally determined activity profiles.

The temperature dependence of the Pgp ATPase activity was also measured in living NIH-MDR1-G185 cells by monitoring the extracellular acidification rate, ECAR (*11*), in the absence and presence of verapamil. Below 35 °C similar Eyring plots were obtained (*33*).

One or More than One Rate-Limiting Transition State? As seen in Figure 1 the Pgp ATPase works (i) under basal conditions (in the absence of drugs), (ii) under conditions of drug-induced activation (at low and intermediate concentrations), and (iii) under conditions of drug-induced inhibition (at high concentrations). To see whether the three different modes of Pgp ATPase activity are rate-limited by the same transition state, we applied the isokinetic equation (eq 5) (*31*) as proposed by Al-Shawi et al. (*19*). The logarithm of the rate constants, ln V_{sw}, measured as a function of the drug concentration at $T_2 = 31$ °C and $T_3 = 37$ °C were plotted as a function of the corresponding rate constants, ln V_{sw}, measured at $T_1 = 25$ °C according to eq 5 (Figure 5). As seen in Figure 5, data fit linear regression lines with a slope, $m \approx 1$ ($m = 0.99$ and $m = 0.90$, respectively). From these data no indication of more than one rate-limiting transition state can be observed, which suggests that the basal, the drug-induced, and the drug-inhibited Pgp ATPase activity are rate-limited by the same transition state.

In a previous investigation (*19*) data for low and high drug concentrations also fell to the same regression line (slope of $m \approx 0.8$), which is close to that in the present analysis. However, the values for basal ATPase activity deviated, and the regression line revealed a slope of $m \approx 0.5$ only. As a consequence two different transition states, one associated with uncoupled basal activity and the other with coupled drug transport activity, were proposed. It should be noted that the investigation was performed with membranes exhibiting different lateral packing densities which might affect the slope of the curve measured under basal conditions (see Discussion).

DISCUSSION

We measured the basal and drug-induced Pgp ATPase activity in inside-out plasma membrane vesicles of NIH-MDR1-G185 cells over a broad concentration range using promazine with low, verapamil with intermediate, and PSC833 with high affinity to the transporter. The activity profile for each drug was measured at different temperatures which allowed assessment of the transition state parameters, $\Delta H^{\ddagger}$, $T\Delta S^{\ddagger}$, and $\Delta G^{\ddagger}$, for Pgp ATPase activity from Eyring plots in the absence and presence of drugs. The relevance of the free energies of activation, $\Delta G^{\ddagger}$, determined was demonstrated by inserting the values into the Eyring equation (eq 2), which yielded the rate constants in excellent agreement with the primary data. In the following we compare the transition state parameters for Pgp ATPase activity in plasma membranes of NIH-MDR1-G185 cells in the absence of drugs with those obtained previously in other systems and analyze the influence of the lateral membrane packing density, π_M. We then discuss the changes in the transition state parameters observed upon titration with the different drugs and estimate to which extent they are due to direct substrate−transporter interactions and to which extent they are membrane mediated. Models for the catalytic cycle of the Pgp ATPase are discussed on the basis of the present data.

The Transition State Parameters for Pgp ATPase Activity in the Absence of Drugs. The transition state parameters for basal Pgp ATPase activity measured in different lipid membranes or membrane mimicking systems (*19, 26*) differ considerably. A meaningful comparison with the transition state parameters for Pgp ATPase activity determined in plasma membranes of NIH-MDR1-G185 cells is possible if data are plotted as a function of the lateral packing density, π_M, of the different membranes or membrane mimicking systems as seen in Figure 6.

The lateral membrane packing density, π_M, is not directly measurable but can be assessed in comparison to the lateral

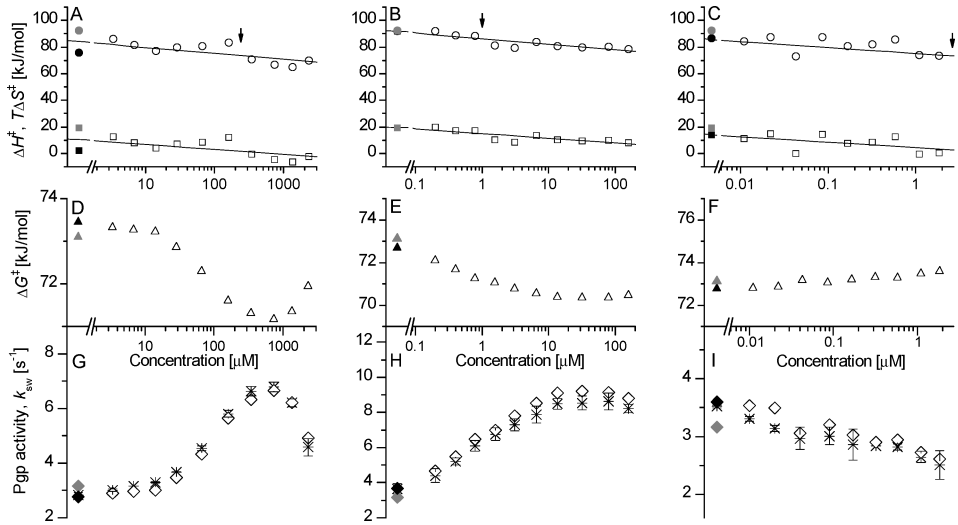

FIGURE 4: The thermodynamic transition state parameters for Pgp ATPase activity in plasma membrane vesicles of NIH-MDR1-G185 cells as a function of drug concentration: promazine (A, D, G), verapamil (B, E, H), and PSC8333 (C, F, I). (A−F) Activation enthalpy, $\Delta H^{\ddagger}$ (●, gray circle, ○); activation entropy, $T\Delta S^{\ddagger}$ (■, gray square, □); and free energy of activation, $\Delta G^{\ddagger}$ (▲, gray triangle, △), at $T = 37$ °C. Filled and open symbols represent data in the absence and presence of drugs, respectively. Filled black and open symbols represent data from one temperature dependence measurement with multiple samples, and filled gray symbols represent the average of seven temperature dependence measurements with multiple samples. (G−I) Measured Pgp ATPase activity at 37 °C (*) (data from Figure 1); Pgp ATPase activity (◆, gray diamond, ◇) calculated according to eq 2 using $\Delta G^{\ddagger}$ values given in panels D−F. The arrows indicate the concentrations of half-maximum activation for verapamil and promazine and the concentration of half-maximum inhibition for PSC833. The straight lines were drawn to guide the eye. For clarity the error bars were omitted. For the activation enthalpy and the activation entropy, the error (representing the goodness of the fit) was ∼20% at very low concentrations and ∼10% at higher concentrations.

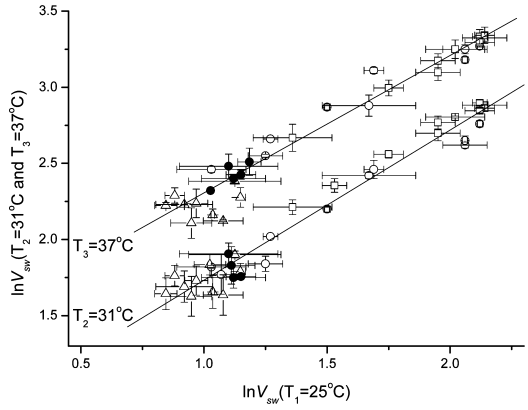

FIGURE 5: Isokinetic relationship. The logarithm of Pgp ATPase activity, ln V_{sw} (at $T_2 = 31$ °C) (lower data set) and ln V_{sw} (at $T_3 = 37$ °C) (upper data set), is plotted as a function of lnV_{sw} (at $T_1 = 25$ °C). Filled symbols (●) basal activity and open symbols drug-induced activity, measured over the whole concentration range given in Figure 1: promazine (○), verapamil (□), and PSC833 (△).

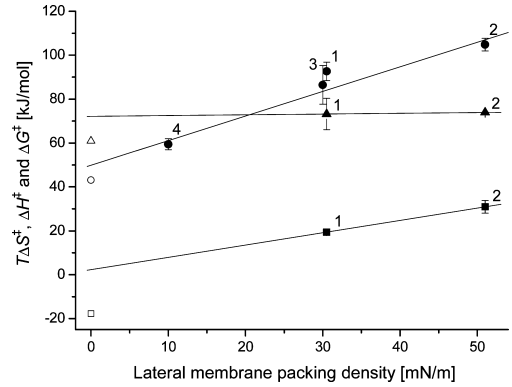

FIGURE 6: The thermodynamic transition state parameters for basal Pgp ATPase activity as a function of the lateral packing density, π_M, of the membrane surrounding the transporter. The lateral membrane packing densities were derived from the concentrations of half-maximum Pgp activation, K_1, determined at pH 7.4 or pH 7.5 according to ref *11*. Different reconstitutions may provide slightly different lateral packing densities. Activation enthalpy, $\Delta H^{\ddagger}$ (●, ○), the product of the absolute temperature and the activation entropy, $T\Delta S^{\ddagger}$ (■, □), and the free energy of activation, $\Delta G^{\ddagger}$, (▲, △) for Pgp ATPase activity at $T = 35$ °C. 1, MDR1 in native NIH-MDR1-G185 membranes (pH 7.0) (present data are an average of seven different temperature dependence measurements with multiple samples); 2, MDR1 in mixed *E. coli* lipids (pH 7.5) (*19*); 3, PGP1 (hamster Pgp), in dimyristoylphosphatidylcholine (*26*), 4, PGP1 in CHAPS (*26*). The open symbols represent the transition state parameters measured for the water-soluble NBD of glucose ABC transporters, GlcV (pH 6.5). It works as a dimer and hydrolyzes one ATP per monomer (*35*). The solid lines are the linear regressions to the data presented as filled symbols.

membrane packing density or surface pressure, π, of a lipid monolayer which is directly measurable. Monolayer−bilayer equivalence packing densities (or equivalence pressures) were obtained by comparing binding isotherms to lipid bilayers with binding isotherms to lipid monolayers at different lateral packing densities (*28*). To assess the lateral packing density, π_M, of a lipid membrane containing the Pgp ATPase, we measured the concentration of half-maximum Pgp ATPase activation, K_1, for verapamil and compared it with the K_1, value for verapamil measured in a membrane with known lateral membrane packing density (for details see ref *11*). For bilayer membranes the lateral packing density varied between $\pi_M \cong 51$ mN/m as estimated for mixed liposomes composed of 60% (w/w) *Escherichia coli* lipids, 17.5% egg phopshatidylcholine, 10% bovine brain phosphatidylserine, and 12.5% cholesterol (*19*) and $\pi_M \cong 30.5 \pm 1.0$ mN/m as estimated for plasma membranes of NIH-MDR1-G185 cells (*11*). For CHAPS micelles the lateral packing density was estimated as $\pi_M \cong 10$ mN/m in analogy to that of SDS micelles (*34*). The extrapolation to zero lateral membrane packing density ($\pi_M = 0$ mN/m) can be considered as the hypothetical situation of Pgp working in an isotropic solvent. For comparison the transition state parameters for ATP

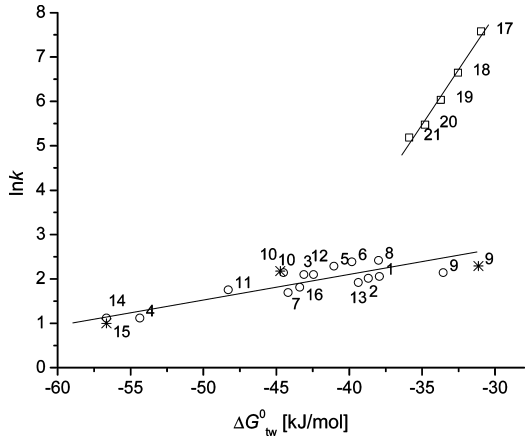

FIGURE 7: Correlation between the rate of substrate transport and substrate affinity to the Pgp ATPase and maltoporin. For the Pgp ATPase the logarithm of the rate constants, k_1, for ATP hydrolysis taken as k is plotted as a function of the free energy of substrate binding from water to the activating binding region of the transporter, $\Delta G°_{tw(1)}$, taken from ref *7* (○). Data obtained from the present investigation are indicated as (∗). Substrates: amitriptyline (1), chlorpromazine (2), *cis*-flupenthixol (3), cyclosporin A (4), dibucaine (5), diltiazem (6), glivec (7), progesterone (8), promazine (9), (*R*/*S*)-verapamil (10), reserpine (11), trifluoperazine (12), triflupromazine (13), OC144-093 (14), PSC833 (15), and vinblastine (16). For comparison, the logarithm of the rate constants, k, for transport across maltoporin is plotted as a function of the free energy of substrate binding from water to maltoporin, $\Delta G°_{tw}$ (□) (*42*): maltotriose (17), maltotetraose (18), maltopentaose (19), maltohexaose (20), and maltoheptaose (21).

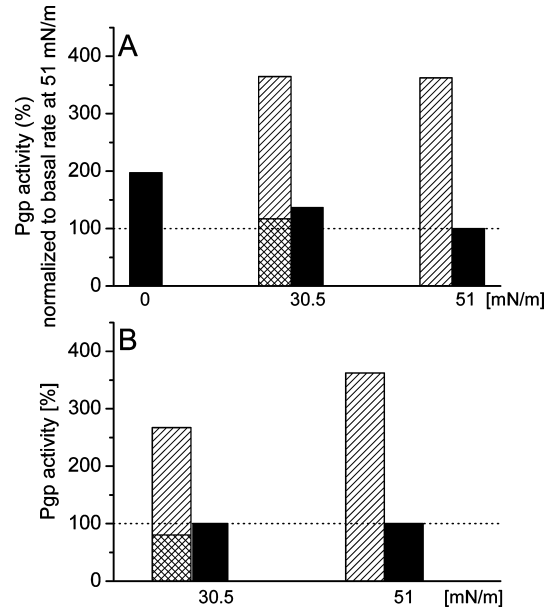

FIGURE 8: The rate of ATP hydrolysis by the Pgp ATPase in membranes with different lateral packing densities. (A) Pgp ATPase activity is normalized to the basal activity in the membrane with the highest lateral packing density, $\pi_M = 51$ mN/m. (B) Pgp ATPase activity is normalized to the basal Pgp ATPase activity at the corresponding lateral membrane packing density. Basal Pgp ATPase activity is shown as black bars and verapamil- and PSC833-stimulated Pgp ATPase activity as hatched and cross-hatched bars, respectively. The Pgp ATPase activity at $\pi_M = 51$ mN/m was calculated from the free energies of activation, $\Delta G^‡$, at $T = 35$ °C according the eq 2; data were taken from ref *19* at pH 7.5. For comparison, the basal and verapamil-induced Pgp ATPase activity was measured at $T = 35$ °C and at pH 7.5 in NIH-MDR1-G185 cell membranes exhibiting an estimated lateral packing density of $\pi_M = 30.5$ mN/m. The Pgp ATPase activity in the presence of PSC833 at $\pi_M = 30.5$ mN/m was calculated from the free energies of activation, $\Delta G^‡$, at $T = 35$ °C according to eq 2. The amount of the Pgp ATPase in the plasma membrane vesicle preparation used in the measurements at pH 7.5 and $T = 35$ °C was estimated as 1.1%.

hydrolysis by the water-soluble NBD of the glucose ABC transporter of the extreme thermoacidophile *Sulfolobus solfataricus*, GlcV (*35*), were included in Figure 6. The soluble NBDs of GlcV dimerize upon ATP binding and hydrolyze both ATP molecules in the interface (*35*).

The free energy of activation for Pgp ATPase activity appears at first sight almost packing density independent. However, it slightly decreases from $\Delta G^‡ = 73.9$ kJ/mol at $\pi_M \cong 51$ mN/m to $\Delta G^‡ = 72.2$ kJ/mol at $\pi_M \cong 0$ mN/m ($\Delta\Delta G^‡ = -1.7$ kJ/mol), which translates into an approximately 2-fold acceleration of ATP hydrolysis. This is in good agreement with previous observations showing that basal Pgp ATPase activity is higher in more disordered lipids with low phase transition temperatures, T_c, than in more ordered lipids with a higher phase transition temperature (see Figure 7 in ref *36*). The free energy of activation, $\Delta G^‡$, has contributions from both enthalpy, $\Delta H^‡$, and entropy, $T\Delta S^‡$; the transporter can thus function either by lowering the enthalpy or enhancing the entropy of activation (i.e., decreasing $-T\Delta S$) (eq 2). In membranes or membrane mimicking systems with the lowest lateral packing density, π_M, the activation entropy, $T\Delta S^‡$, is close to zero and the Pgp ATPase thus functions in an essentially enthalpy-driven manner. A similar situation is observed for the soluble NBDs of GlcV (*35*), which is also enthalpy-driven. With increasing lateral membrane packing density, π_M, the enthalpy, $\Delta H^‡$, and the entropy, $T\Delta S^‡$, contribution increase and the latter becomes significant. This suggests that the lipid membrane plays a crucial role in the mode of activation of the Pgp ATPase. The function of proteins embedded in densely packed lipid bilayers may thus be supported by the high "entropy-producing potential" of lipid membranes as suggested previously (*37*).

All over, the activation energy, E_a, and activation enthalpy, $\Delta H^‡$, for Na/K-ATPase seem to be smaller than those of the Pgp ATPase. The activation energy was determined as $E_a \approx 19$ kJ/mol for the Na/K-ATPase in the foot muscle of land snails (*38*). The activation enthalpy was determined as $\Delta H^‡ \approx 67$ kJ/mol and $\Delta H^‡ \approx 74$ kJ/mol for the Na/K-ATPase from the shark rectal gland reconstituted into dioleoylphosphatidylcholine and into dioleoylphosphatidylcholine containing 40% cholesterol, respectively (*39*). Land snail membranes with a high content of highly unsaturated lipids (*40*) exhibit most likely the lowest lateral packing density, membranes formed from dioleoylphosphatidylcholine exhibit an intermediate, and the cholesterol-containing membranes the highest lateral packing density of the three membranes cited. Provided the Na/K-ATPases from the different sources are comparable, the activation energy, E_a, seems again to increase with the lateral packing density of the membrane. For the sarcoplasmic reticulum Ca-ATPase it was shown that the lipid fluidity directly modulates the overall protein rotational mobility and the ATPase activity (*41*), which again supports the trends observed in Figure 6.

The Transition State Parameters as a Function of the Drug Affinity to the Transporter and Drug Concentration. Figure 7 displays the drug-induced Pgp ATPase activity in plasma membrane vesicles formed from NIH-MDR1-G185 cells, ln k_1 (indicated as ln k in Figure 7), as a function of the binding affinity of the drug to the transporter (i.e., the free energy of drug binding from water to the transporter,$\Delta G°_{tw(1)}$) for

promazine, verapamil, and PSC833 in comparison to other compounds measured previously under the same conditions (*7*). The Pgp ATPase activity, ln k_1, decreases linearly with increasing affinity of the drug from water to the transporter (or decreasing free energy of drug binding from water to the transporter, $\Delta G^\circ_{tw(1)}$). A similar linear correlation between the rate constant, ln k, and the affinity to the transport system was observed previously for maltoporin LamB of *E. coli* (*42*) as shown for comparison in Figure 7. Maltoporin is a much simpler transport system which allows the translocation of maltodextrins of different lengths.

Maltodextrins interact with maltoporin essentially via transient hydrogen bond formation, whereby the substrates provide the hydrogen bond donor groups and the transporter the hydrogen bond acceptor groups (*42*). A related mechanism has been proposed for the interaction of the Pgp ATPase with transport substrates. However, in the case of the Pgp ATPase the substrate provides the hydrogen bond acceptor groups and Pgp the hydrogen bond donor groups (*4, 11, 43*). It is interesting to note that the overall rate of translocation by maltoporin is in the millisecond range, whereas the rate of substrate translocation by Pgp is in the range of seconds. The low rate of transport by the Pgp ATPase seems to be due to the requirement for a conformational switch between the binding- and the release-competent conformation, respectively.

According to the Eyring equation (eq 2) the rate, k, decreases with increasing free energy of activation, $\Delta G^\ddagger$. Figure 7 thus suggests that the free energy of activation, $\Delta G^\ddagger$, for Pgp ATPase activity increases with increasing substrate affinity to the transporter (or decreasing free energy of activation, $\Delta G^\circ_{tw(1)}$). PSC833, the compound with the highest affinity to the transporter, indeed shows the highest activation energy, $\Delta G^\ddagger$, as seen in Table 1.

In addition to the drug affinity, the drug concentration also plays a substantial role for the Pgp ATPase activity (Figure 1 and Figure 4G−I) and the corresponding free energy of activation, $\Delta G^\ddagger$ (Figure 4D−F). The change in the free energy of activation varied from $\Delta\Delta G^\ddagger \sim -3.8\%$ to $\Delta\Delta G^\ddagger \sim +0.7\%$. The activation enthalpy, $\Delta H^\ddagger$, and the activation entropy, $T\Delta S^\ddagger$, for the Pgp ATPase activity in NIH-MDR1-G185 plasma membranes decreased with increasing concentration for both activating and inhibitory compounds as seen in Figure 4A−C. At the highest concentrations measured the reduction in the enthalpy, $\Delta\Delta H^\ddagger$, increased in the order verapamil < PSC833 < promazine. However, if the compounds are compared at identical concentrations, the "inhibitor" PSC833 has the strongest and promazine the weakest enthalpy lowering effect. The strong effect of promazine at the high concentrations measured (Figure 4A−C) may be 2-fold. First, more than one molecule of the drug may be bound to the transporter and the transporter may thus feel a cargo of "higher affinity". The low activation entropy in the presence of more than one molecule with low affinity or of one molecule with high affinity may be due to a loss of residual motion of the substrate−transporter complex. Moreover, the high drug concentration in the membrane (in the case of promazine) may slightly lower the order parameter and the lateral packing density of the membrane.

The Lateral Packing Density of the Membrane May Vary in the Course of the Experiment. Drug partitioning into membranes leads to a reduction of the fatty acyl chain order of lipids and a concomitant decrease of the lateral lipid packing density, π_M, of the membrane, as has been shown by deuterium NMR for verapamil (*44*), local anesthetics (*45*), and also for cyclosporin A, an analogue of PSC833, however, to a lesser extent (*46*). Since the mole fraction of drugs in the lipid membrane at the concentrations of half-maximum Pgp ATPase activation is rather high (*11*), a reduction of the membrane order and the lateral membrane packing density can be expected for most drugs.

The fatty acyl chain order of lipid bilayers and the lateral packing density of the lipid bilayer, π_M, also decrease with increasing temperature as shown by deuterium NMR (*47*). In the limited temperature intervals, ΔT, the lateral membrane packing density changes may, however, be small as suggested by the apparently linear Arrhenius or Eyring plots for Pgp ATPase activity ($\Delta T = 18$ °C for crude membrane preparations of Chinese hamster ovary cells, CR1R12 (*5*), $\Delta T = 17$ °C for HeLa cells (*22*), and $\Delta T = 12$ °C for proteoliposomes (*19*) and plasma membrane of NIH-MDR1-G185 cells (present investigation)). A much broader temperature range ($\Delta T = 40$ °C) was accessible by using radioactively labeled ATP and yielded a convex Arrhenius plot for the Pgp ATPase in crude membranes of CH^RB30 (*25*). It is interesting to note that if the activation energy, E_a, for crude membranes of CH^RB30 (*25*) is assessed in the temperature range used in the present investigation, a comparable value is obtained. The water-soluble NBD of the glucose ABC transporter of the extreme thermoacidophile *S. solfataricus*, GlcV, shows in contrast an Eyring plot which is linear over a much broader temperature range ($\Delta T = 60$ °C) (*35*). Nevertheless, the change in the lipid packing density with temperature may not be the only factor responsible for the nonlinear Eyring plot of the Pgp ATPase.

Differentiation between Drug-Induced and Packing Density-Induced Effects. As discussed, the enthalpy of activation, $\Delta H^\ddagger$, for Pgp ATPase activity decreases with decreasing lateral membrane packing density, π_M (Figure 6), as well as with increasing drug concentration (Figure 4A−C). The question arises to which extent the decrease in the activation enthalpy in the present experiments is due to a drug-induced reduction in the membrane packing density, π_M, and to which extent it is due to the direct drug−transporter interaction. To address this question in more detail, we compared the basal rates of ATP hydrolysis with the drug-induced rates, both measured at different lateral membrane packing densities (Figure 8A). In Figure 8A all data are given relative to the basal rate at the highest lateral packing density, taken as 100%. The comparison in Figure 8A reveals that the maximum possible acceleration achieved by loosening the lateral membrane packing density, π_M, is lower than that induced by concentrations of verapamil yielding the maximum activity, V_1, but higher than the effect induced by the inhibitory PSC833. This implies that a significant part of the activity modulating effect of drugs is due to the direct substrate−transporter interaction and that the acceleration of ATP hydrolysis due to drug-induced membrane loosening is small. Figure 8A moreover reveals that a specific drug (e.g., verapamil) induces approximately the same rate of ATP hydrolysis in different membranes if compared to a single reference state, (e.g., the basal rate at the highest lateral packing density). This further supports the assumption that the substrate transporter interaction is independent of the lateral membrane packing density (*11*). Generally, drug-induced Pgp ATPase activity is expressed relative to the basal activity in the respective system as shown in Figure 8B. This representation gives

the impression that the Pgp ATPase works better in densely packed than in loosely packed membranes which is misleading (for review see also Introduction in ref *48*). A comparable situation is seen in Figure 3 which shows a decrease of the fold activity with increasing temperature, due to the fact that the basal activity shows stronger temperature dependence than the drug-induced activity.

Discussion of the Catalytic Cycle: Does Drug Transport Occur before or after ATP Hydrolysis by the Pgp ATPase? We first consider the Pgp ATPase as a simple enzyme, ignoring its transport function. Under these conditions ATP is the substrate which is transformed to inorganic phosphate and ADP. For this reaction three transition states can be assumed, one for ATP binding (with the free energy of activation, $\Delta G^{\ddagger}_1$), a second one for ATP hydrolysis (with the free energy of activation, $\Delta G^{\ddagger}_2$), and a third one for ADP release (with the free energy of activation, $\Delta G^{\ddagger}_3$), whereby the second step is rate-limiting ($\Delta G^{\ddagger}_2 \gg \Delta G^{\ddagger}_1$ and $\Delta G^{\ddagger}_3$). The free energies of ATP binding and ATP hydrolysis are similar[2] and are dissipated. The energy levels of the substrate decrease from one step to the other, whereas the energy level of the enzyme remains unchanged. A model with a rate-limiting ATP hydrolysis step could also be considered in the presence of a transport substrate (i.e., a drug) which lowers the activation energy, $\Delta G^{\ddagger}_2$. If we assume that this model is appropriate for the Pgp ATPase, drugs must still be bound when the transition state for ATP hydrolysis has formed and drugs are released only after ATP is hydrolyzed. On the basis of the apparent linearity of Eyring plots an analogous model was suggested by Al-Shawi et al. (*19*).

A different interpretation is possible if we assume a model analogous to that proposed previously for Na,K-ATPases (*50*) and adopted for the Pgp ATPase by Higgins and Linton (*21*). In this model ATP binding and hydrolysis serve to switch the protein between two conformational states with a high- and a low-affinity binding site for the substrate, respectively. The free energy of ATP binding and ATP hydrolysis may be transformed into potential energy which is stored in the protein and is then used to drive the two conformational changes. If we further assume that the two conformational changes of the Pgp ATPase exhibit similar free energies of activation, $\Delta G^{\ddagger}$, the transition state for the first conformational change could be modulated by the presence of drugs, and drugs could then be released before the ATP-driven resetting step occurs. On the basis of the observation that the rate of ATP hydrolysis depends in an exponential manner on the drug affinity to the transporter (Figure 7), we previously suggested that drugs may be released before ATP is hydrolyzed (*7*), which is consistent with the second model. However, for a conclusive answer, further experiments are required.

[2] Based on the previously measured Michaelis−Menten constants, K_m (*23*), and eq 8, the free energy of ATP binding from water to the transporter, ΔG°_b, was estimated as $\Delta G^{\circ}_{ATP,b} \approx -31.1$ kJ/mol and $\Delta G^{\circ}_{ATP,b} \approx -30.1$ kJ/mol in the presence and absence of drugs, respectively. The free energy of drug binding from water to the activating binding regions of the transporter was estimated as $\Delta G^{\circ}_{tw(1)} \approx -30$ to -54 kJ/mol and the free energy of drug binding from the lipid bilayer to the activating binding region of the transporter as $\Delta G^{\circ}_{tl(1)} \approx -7$ to -27 kJ/mol (*11*). It should be noted that the Michaelis−Menten constants and the dissociation constants are similar for ATP (*49*) as well as for substrates (*14*). Under physiological conditions the free energy of ATP hydrolysis is $\Delta G^{\circ}_{ATP,h} = -55$ kJ/mol (*50*).

Summary. To test how Pgp senses its substrates, we measured the temperature dependence of the Pgp ATPase activity in inside-out plasma membrane vesicles of NIH-MDR1-G185 cells over a broad concentration range using three drugs with different affinities to the transporter and determined the transition state parameters from Eyring plots in the temperature range, $\Delta T = 25-37$ °C. To investigate how the Pgp senses the lipid composition of the membrane, we compared the transition state parameters for basal ATPase activity in inside-out plasma membrane vesicles of NIH-MDR1-G185 cells with the transition state parameters for Pgp ATPase activity in other systems exhibiting different lateral membrane packing densities, π_M. This revealed that the free energy of activation, $\Delta G^{\ddagger}$, decreases slightly with decreasing lateral membrane packing density, π_M (corresponding to a maximally 2-fold increase in activity). Moreover, it revealed that the transporter works in an essentially enthalpy-driven manner at low and in a more entropy-driven manner at high lateral packing densities.

Addition of low-affinity drugs at low and intermediate concentrations lead to a small decrease (maximally $\Delta\Delta G^{\ddagger} = \sim -3.8\%$) in the free energy of activation, $\Delta G^{\ddagger}$, relative to basal values (corresponding to an increase in ATPase activity). Addition of high-affinity drugs at low concentrations, or low-affinity drugs at high concentrations, lead, in contrast, to a small increase ($\Delta\Delta G^{\ddagger} = \sim +0.7\%$) in the free energy of activation, $\Delta G^{\ddagger}$ (corresponding to a decrease in the rate of transport). The activation enthalpy, $\Delta H^{\ddagger}$ (or activation energy E_a), and the activation entropy, $T\Delta S^{\ddagger}$, decreased significantly with increasing concentration and increasing transporter affinity of the drug. At high drug concentrations the Pgp ATPase worked in an essentially enthalpy-driven manner which may be due to the loss of residual motion of the transporter and, however, to lower extent, to the loosening of the lateral membrane packing density upon drug partitioning into the membrane.

Basal activity seems to increase slightly with decreasing lateral packing density, π_M, but the effective transport rate seems not to decrease. The Pgp ATPase is thus able to efficiently transport cargo of considerable size at almost constant rate in membranes of different lateral packing densities, π_M, whereas uncatalyzed flip-flop and diffusion of molecules across a lipid membrane decrease exponentially with increasing lateral packing density, π_M, and increasing cross-sectional area, A_D (*13, 29*). Densely packed lipid membranes, expressing a high level of the Pgp ATPase thus guarantee excellent barrier properties.

ACKNOWLEDGMENT

We thank Joachim Seelig and Dagmar Klostermeier for helpful discussions.

REFERENCES

1. Glavinas, H., Krajcsi, P., Cserepes, J., and Sarkadi, B. (2004) The role of ABC transporters in drug resistance, metabolism and toxicity. *Curr. Drug Deliv. 1*, 27–42.
2. Gottesman, M. M., Ludwig, J., Xia, D., and Szakacs, G. (2006) Defeating drug resistance in cancer. *Disco. Med. 6*, 18–23.
3. Rosenberg, M. F., Callaghan, R., Modok, S., Higgins, C. F., and Ford, R. C. (2005) Three-dimensional structure of P-glycoprotein: the transmembrane regions adopt an asymmetric configuration in the nucleotide-bound state. *J. Biol. Chem. 280*, 2857–2862.

4. Seelig, A. (1998) A general pattern for substrate recognition by P-glycoprotein. *Eur. J. Biochem. 251*, 252–261.
5. Litman, T., Zeuthen, T., Skovsgaard, T., and Stein, W. D. (1997) Structure-activity relationships of P-glycoprotein interacting drugs: kinetic characterization of their effects on ATPase activity. *Biochim. Biophys. Acta 1361*, 159–168.
6. Al-Shawi, M. K., and Senior, A. E. (1993) Characterization of the adenosine triphosphatase activity of Chinese hamster P-glycoprotein. *J. Biol. Chem. 268*, 4197–4206.
7. Aanismaa, P., and Seelig, A. (2007) P-glycoprotein kinetics measured in plasma membrane vesicles and living cells. *Biochemistry 46*, 3394–3404.
8. Gorbulev, S., Abele, R., and Tampe, R. (2001) Allosteric crosstalk between peptide-binding, transport, and ATP hydrolysis of the ABC transporter TAP. *Proc. Natl. Acad. Sci. U.S.A. 98*, 3732–3737.
9. Raviv, Y., Pollard, H. B., Bruggemann, E. P., Pastan, I., and Gottesman, M. M. (1990) Photosensitized labeling of a functional multidrug transporter in living drug-resistant tumor cells. *J. Biol. Chem. 265*, 3975–3980.
10. Shapiro, A. B., and Ling, V. (1997) Extraction of Hoechst 33342 from the cytoplasmic leaflet of the plasma membrane by P-glycoprotein. *Eur. J. Biochem. 250*, 122–129.
11. Gatlik-Landwojtowicz, E., Aanismaa, P., and Seelig, A. (2006) Quantification and characterization of P-glycoprotein-substrate interactions. *Biochemistry 45*, 3020–3032.
12. Ambudkar, S. V., Cardarelli, C. O., Pashinsky, I., and Stein, W. D. (1997) Relation between the turnover number for vinblastine transport and for vinblastine-stimulated ATP hydrolysis by human P-glycoprotein. *J. Biol. Chem. 272*, 21160–21166.
13. Seelig, A. (2007) The role of size and charge for blood-brain barrier permeation of drugs and fatty acids. *J. Mol. Neurosci. 33*, 32–41.
14. Lu, P., Liu, R., and Sharom, F. J. (2001) Drug transport by reconstituted P-glycoprotein in proteoliposomes. Effect of substrates and modulators, and dependence on bilayer phase state. *Eur. J. Biochem. 268*, 1687–1697.
15. Omote, H., and Al-Shawi, M. K. (2002) A novel electron paramagnetic resonance approach to determine the mechanism of drug transport by P-glycoprotein. *J. Biol. Chem. 277*, 45688–45694.
16. Senior, A. E., Al-Shawi, M. K., and Urbatsch, I. L. (1995) The catalytic cycle of P-glycoprotein. *FEBS Lett. 377*, 285–289.
17. Chen, M., Abele, R., and Tampe, R. (2003) Peptides induce ATP hydrolysis at both subunits of the transporter associated with antigen processing. *J. Biol. Chem. 278*, 29686–29692.
18. Seelig, A., and Gatlik-Landwojtowicz, E. (2005) Inhibitors of multidrug efflux transporters: their membrane and protein interactions. *Mini. Rev. Med. Chem. 5*, 135–151.
19. Al-Shawi, M. K., Polar, M. K., Omote, H., and Figler, R. A. (2003) Transition state analysis of the coupling of drug transport to ATP hydrolysis by P-glycoprotein. *J. Biol. Chem. 278*, 52629–52640.
20. Qu, Q., Chu, J. W., and Sharom, F. J. (2003) Transition state P-glycoprotein binds drugs and modulators with unchanged affinity, suggesting a concerted transport mechanism. *Biochemistry 42*, 1345–1353.
21. Higgins, C. F., and Linton, K. J. (2004) The ATP switch model for ABC transporters. *Nat. Struct. Mol. Biol. 11*, 918–926.
22. Sauna, Z. E., and Ambudkar, S. V. (2001) Characterization of the catalytic cycle of ATP hydrolysis by human P-glycoprotein. The two ATP hydrolysis events in a single catalytic cycle are kinetically similar but affect different functional outcomes. *J. Biol. Chem. 276*, 11653–11661.
23. Kerr, K. M., Sauna, Z. E., and Ambudkar, S. V. (2001) Correlation between steady-state ATP hydrolysis and vanadate-induced ADP trapping in human P-glycoprotein. Evidence for ADP release as the rate-limiting step in the catalytic cycle and its modulation by substrates. *J. Biol. Chem. 276*, 8657–8664.
24. Sauna, Z. E., Smith, M. M., Muller, M., and Ambudkar, S. V. (2001) Functionally similar vanadate-induced 8-azidoadenosine 5′-[alpha-(32)P]Diphosphate-trapped transition state intermediates of human P-glycoprotin are generated in the absence and presence of ATP hydrolysis. *J. Biol. Chem. 276*, 21199–21208.
25. Buxbaum, E. (1999) Co-operating ATP sites in the multiple drug resistance transporter Mdr1. *Eur. J. Biochem. 265*, 54–63.
26. Romsicki, Y., and Sharom, F. J. (1998) The ATPase and ATP-binding functions of P-glycoprotein-modulation by interaction with defined phospholipids. *Eur. J. Biochem. 256*, 170–178.
27. Omote, H., Figler, R. A., Polar, M. K., and Al-Shawi, M. K. (2004) Improved energy coupling of human P-glycoprotein by the glycine 185 to valine mutation. *Biochemistry 43*, 3917–3928.
28. Seelig, A. (1987) Local anesthetics and pressure: a comparison of dibucaine binding to lipid monolayers and bilayers. *Biochim. Biophys. Acta 899*, 196–204.
29. Fischer, H., Gottschlich, R., and Seelig, A. (1998) Blood-brain barrier permeation: molecular parameters governing passive diffusion. *J. Membr. Biol. 165*, 201–211.
30. Gatlik-Landwojtowicz, E., Aanismaa, P., and Seelig, A. (2004) The rate of P-glycoprotein activation depends on the metabolic state of the cell. *Biochemistry 43*, 14840–14851.
31. Exner, O. (1973) The enthaly-entropy relationship. *Prog. Phys. Org. Chem. 10*, 411–482.
32. Cantor, C. R., and Schimmel, P. R. (1980) *Biophysical Chemistry, Part I: The conformation of biological macromolecules*, Vol. 1, p 283, W. H. Freeman and Co., San Francisco.
33. Landwojtowicz, E. (2002) Multidrug transporter P-glycoprotein: From kinetics of drug-induced ATPase activation in intact cells to structure-activity relationships, in *Biozentrum*, p 121, University of Basel, Basel.
34. Seelig, A. (1992) Interaction of a substance P agonist and of substance P antagonists with lipid membranes. A thermodynamic analysis. *Biochemistry 31*, 2897–2904.
35. Pretz, M. G., Albers, S. V., Schuurman-Wolters, G., Tampé, R., Driessen, A. J., and van der Does, C. (2006) Thermodynamics of the ATPase cycle of GlcV, the nucleotide-binding domain of the glucose ABC transporter of *Sulfolobus solfataricus*. *Biochemistry 45*, 15056–15067.
36. Doige, C. A., Yu, X., and Sharom, F. J. (1993) The effects of lipids and detergents on ATPase-active P-glycoprotein. *Biochim. Biophys. Acta 1146*, 65–72.
37. Seelig, J., and Ganz, P. (1991) Nonclassical hydrophobic effect in membrane binding equilibria. *Biochemistry 30*, 9354–9359.
38. Ramnanan, C. J., and Storey, K. B. (2006) Suppression of Na^+/K^+-ATPase activity during estivation in the land snail *Otala lactea*. *J. Exp. Biol. 209*, 677–688.
39. Cornelius, F. (2001) Modulation of Na,K-ATPase and Na-ATPase activity by phospholipids and cholesterol. I. Steady-state kinetics. *Biochemistry 40*, 8842–8851.
40. Zhu, N., Dai, X., Lin, D. S., and Connor, W. E. (1994) The lipids of slugs and snails: evolution, diet and biosynthesis. *Lipids 29*, 869–875.
41. Squier, T. C., Bigelow, D. J., and Thomas, D. D. (1988) Lipid fluidity directly modulates the overall protein rotational mobility of the Ca-ATPase in sarcoplasmic reticulum. *J. Biol. Chem. 263*, 9178–9186.
42. Andersen, C., Jordy, M., and Benz, R. (1995) Evaluation of the rate constants of sugar transport through maltoporin (LamB) of *Escherichia coli* from the sugar-induced current noise. *J. Gen. Physiol. 105*, 385–401.
43. Seelig, A., Blatter, X. L., and Wohnsland, F. (2000) Substrate recognition by P-glycoprotein and the multidrug resistance-associated protein MRP1: a comparison. *Int. J. Clin. Pharmacol. Ther. 38*, 111–121.
44. Meier, M., Blatter, X. L., Seelig, A., and Seelig, J. (2006) Interaction of verapamil with lipid membranes and P-glycoprotein: connecting thermodynamics and membrane structure with functional activity. *Biophys. J. 91*, 2943–2955.
45. Auger, M., Jarrell, H. C., and Smith, I. C. (1988) Interactions of the local anesthetic tetracaine with membranes containing phosphatidylcholine and cholesterol: a ^2H NMR study. *Biochemistry 27*, 4660–4667.
46. Schote, U., Ganz, P., Fahr, A., and Seelig, J. (2002) Interactions of cyclosporines with lipid membranes as studied by solid-state nuclear magnetic resonance spectroscopy and high-sensitivity titration calorimetry. *J. Pharm. Sci. 91*, 856–867.
47. Seelig, A., and Seelig, J. (1977) Effect of a single cis double bond on the structures of a phospholipid bilayer. *Biochemistry 16*, 45–50.
48. Seelig, A., and Gerebtzoff, G. (2006) Enhancement of drug absorption by noncharged detergents through membrane and P-glycoprotein binding. *Expert Opin. Drug Metab. Toxicol. 2*, 733–752.
49. Sharom, F. J., Liu, R., Romsicki, Y., and Lu, P. (1999) Insights into the structure and substrate interactions of the P-glycoprotein multidrug transporter from spectroscopic studies. *Biochim. Biophys. Acta 1461*, 327–345.
50. Läuger, P., Ed. (1991) *Electrogenic Ion Pumps*, Sinauer, Sunderland, MA.

BI800209H